Synapsins as major neuronal Ca^{2+}/S100A1-interacting proteins

Jörg HEIERHORST*[1], Ken I. MITCHELHILL*, Richard J. MANN*, Tony TIGANIS*, Andrew J. CZERNIK†, Paul GREENGARD† and Bruce E. KEMP*

*St. Vincent's Institute of Medical Research, 41 Victoria Parade, Fitzroy, VIC 3065, Australia, and †Laboratory of Molecular and Cellular Neuroscience, The Rockefeller University, 1230 York Avenue, New York, NY 10021, U.S.A.

The mammalian S100A1 protein can activate the invertebrate myosin-associated giant protein kinase twitchin in a Ca^{2+}-dependent manner by more than 1000-fold *in vitro*; however, no mammalian S100-dependent protein kinases are known. In an attempt to identify novel mammalian Ca^{2+}/S100A1-regulated protein kinases, brain extracts were subjected to combined Ca^{2+}-dependent affinity chromatography with S100A1 and an ATP analogue. This resulted in the purification to near-homogeneity of the four major synapsin isoforms Ia, Ib, IIa and IIb. All four synapsins were specifically affinity-labelled with the ATP analogue 5′-*p*-fluorosulphonylbenzoyladenosine. S100A1 bound to immobilized synapsin IIa in BIAcore experiments in a Ca^{2+}-dependent and Zn^{2+}-enhanced manner with submicromolar affinity; this interaction could be competed for with synthetic peptides of the proposed S100A1-binding sites of synapsin. Double-labelling confocal immunofluorescence microscopy demonstrated that synapsins and S100A1 are both present in the soma and neurites of PC12 cells, indicating their potential to interact in neurons *in vivo*.

Key words: EF hand, kinase, neuron, PC12 cells.

INTRODUCTION

The S100 family comprises at least 17 proteins [1]. Most of these are dimeric and bind Ca^{2+} ions to EF-hand domains; they can also bind Zn^{2+}. Several proteins to which S100 proteins can bind in a Ca^{2+}-dependent manner have been reported; however, only few of these are enzymes regulated by this interaction [1,2]. We have recently demonstrated that the dimeric S100A1 protein can activate the invertebrate myosin-associated protein kinase twitchin in a Ca^{2+}-dependent and Zn^{2+}-enhanced manner by more than 1000-fold [3]. Ca^{2+}/S100A1 binds to the autoinhibitory sequence of twitchin kinase, thereby opening the active site for substrate access and catalytic activity, an activation mechanism similar to that proposed for Ca^{2+}/calmodulin-dependent protein kinases [4]. This indicated that the S100A1 protein has the potential to act as a Ca^{2+}-dependent protein kinase activator similar to calmodulin.

We tried to identify mammalian Ca^{2+}/S100A1-regulated protein kinases. Any such kinase should have the following two properties: first, it should interact with S100 proteins in a Ca^{2+}-dependent manner; secondly, it should bind ATP or nucleotide analogues. S100A1 is expressed most abundantly in neurons, kidney, and cardiac and skeletal muscle cells. We used brain extracts in combined Ca^{2+}-dependent affinity chromatography experiments with S100A1 and an ATP analogue. Surprisingly, this led to the identification of the synapsin isoforms Ia/b and IIa/b as major Ca^{2+}/S100A1-binding proteins in the brain.

Synapsins are the most abundant synaptic vesicle-associated proteins and have a crucial role in the regulation of neurotransmitter release and synaptogenesis [5–9]. Synapsin I, synapsin II and I/II double-knock-out mice exhibit impaired synaptic transmission when stimulated at high frequency, a decreased density of synaptic vesicles in the active zone of synaptic terminals, and an increased incidence of seizures triggered by sensory stimulation [7,8]. In lower vertebrates, synapsin is required for the availability of a distal reserve pool of synaptic vesicles, the absence of which also results in depressed synaptic transmission after high-frequency stimulation [10]. Finally, synapsin also seems to have a similar role in regulating the distal vesicle pool in the squid giant axon; however, there it might also directly regulate the release process [11]. The molecular mechanism of the regulation of transmitter release by synapsins is currently unclear and it is not known whether and how several proteins that bind synapsins with high affinity (e.g. actin, tubulin, calmodulin, Src and Grb2) are involved in this function.

EXPERIMENTAL

Protein expression

Recombinant rat S100A1 was expressed in *Escherichia coli* and purified as described [12]. Synapsin IIa was expressed in Sf9 (*Spodoptera frugiperda*) cells using the baculovirus system and partly purified by differential centrifugation and extraction from the membrane fraction as described [13], and then further purified by Ca^{2+}/S100A1-affinity chromatography and Blue-Sepharose chromatography as described below.

Affinity chromatography of brain lysates

Rat brains (5–10) were homogenized in 5 vol. of 150 mM NaCl/20 mM Tris/HCl (pH 7.4)/5 mM magnesium acetate/1 mM $CaCl_2$/0.1 mM $ZnCl_2$/0.05% (v/v) Tween 20/5 μg/ml aprotinin/1 μg/ml leupeptin/1 mM benzamidine/1 mM PMSF and centrifuged at 16000 ***g*** for 30 min. The supernatant was loaded on a S100A1-affinity column [5 mg of S100A1 immobilized on a 1 ml *N*-hydroxysuccinimide-activated HiTrap

Abbreviations used: FSBA, 5′-*p*-fluorosulphonylbenzoyladenosine; NGF, nerve growth factor.

[1] To whom correspondence should be addressed (e-mail heier@ariel.its.unimelb.edu.au).

column (Pharmacia) in accordance with the supplier's instructions] at a flow rate of up to 0.5 ml/min. The column was washed with 6 ml of the same buffer but lacking protease inhibitors and was eluted with 150 mM NaCl/20 mM Tris/HCl (pH 7.4)/5 mM magnesium acetate/5 mM EGTA. Peak fractions were pooled, loaded on an approx. 0.5 ml Blue-Sepharose (Pharmacia) column that had been washed with PBS containing 10 mM magnesium acetate, before it was eluted with 2 M NaCl/10 mM sodium phosphate (pH 7.4)/10 mM magnesium acetate. Peak fractions were pooled, dialysed against 10 mM Tris/HCl, pH 7.4, and concentrated by using Centricon membranes.

Protein microsequence analysis

After SDS/PAGE, slices containing the proteins to be identified were excised from Coomassie-stained gels and subjected to proteolysis *in situ* with trypsin as described [14]. Eluted peptides were subjected to chromatography on Nucleosil C_{18} (5 μm bead size, 300 Å pore size) reversed-phase material packed in a 1 mm × 250 mm glass-lined column (SGE) on a Pharmacia SMART system with a linear 0–80 % (v/v) acetonitrile/0.1 % trifluoroacetic acid gradient over 120 min at 40 μl/min. Proteins were monitored at 214 nm and peaks were collected manually. Peptides were subjected to mass analysis with a PerSeptive Biosystems Voyager DE mass spectrometer (matrix-assisted laser desorption ionization–time-of-flight MS) and sequenced with a Hewlett Packard G1000A Protein Sequencer as described [14].

Labelling experiments with 5′-*p*-fluorosulphonylbenzoyladenosine (FSBA)

Protein samples were incubated for 30 min at 30 °C in 10 mM Tris/HCl, pH 7.4, with 250 μM FSBA (Boehringer or Sigma) and 2.5 % (v/v) DMSO. Where indicated, $CaCl_2$ was added to 2 mM, and S100A1 to 1 μM. In competition experiments, adenosine or nucleotides were added at 1 mM. After SDS/PAGE and transfer on PVDF membranes, reaction products were analysed in immunoblot experiments with an anti-FSBA antibody contained in the ATP-binding protein detection kit (Boehringer Mannheim).

Surface plasmon resonance experiments

Purified synapsin IIa (125 μg/ml in 20 mM sodium acetate, pH 4.5) was injected at 5 μl/min on *N*-hydroxysuccinimide/*N*-ethyl-*N*′-(3-diethylaminopropyl)carbodi-imide-activated CM5-sensor chips to yield an immobilized level of 800 response units for kinetic measurements or 6000 response units for some other experiments. The buffer for binding experiments was 150 mM NaCl/20 mM Tris/HCl (pH 7.4)/5 mM magnesium acetate/0.005 % (v/v) Tween 20/1 mM $CaCl_2$/100 μM $ZnCl_2$; in respective control experiments either Zn^{2+} or Ca^{2+} was omitted. S100A1, at the concentrations indicated in the figure legends, was injected at flow rates of 5 μl/min in routine experiments, 2 μl/min in equilibrium binding experiments and 100 μl/min in kinetic experiments. After the initial dissociation phase, remaining S100A1 was eluted in the same buffer containing 5 mM EGTA instead of Ca^{2+} and Zn^{2+}. Response values were corrected for refractive index change by subtraction of responses measured at the same time on a mock-derivatized channel.

Affinity constants were derived from the relationship:

$$R_{eq}/C = K_a R_{max} - K_a R_{eq}$$

where R_{eq} and R_{max} are the equilibrium and maximum response levels respectively (BIAtechnology Handbook and BIAevaluation 2.1 Software Handbook; Pharmacia Biosensor AB). For determination of synapsin (124–145) and synapsin (311–337) peptide affinities, 35 μl of sample containing 1 μM S100A1 and various concentrations of peptide were incubated at 15 °C for 2 h before injection. Concentrations of free S100A1 were determined from comparison with a standard curve of S100A1 ranging from 32 nM to 1 μM. The dissociation constants for the binding of synapsin peptides to S100A1 in solution were obtained by Scatchard analysis as described previously [15,16]. In our system the Scatchard transformation yields:

$$[B_{S100}]/[F_{S100}] = 1/K_d \times [F_{synapsinpeptide}]$$

Tissue culture

PC12 cells were maintained in Dulbecco's modified Eagle's medium containing 10 % (v/v) fetal calf serum and 5 % (v/v) horse serum. For differentiation, Dulbecco's modified Eagle's medium was used with 1 % (v/v) horse serum and 80 μg/ml nerve growth factor (NGF; Gibco BRL). For immunoblotting experiments, cells were grown in plastic dishes and lysed in RIPA buffer. For immunofluorescence, cells were grown on coverslips coated with 2 % (w/v) collagen. Before fixation with 3.2 % (w/v) paraformaldehyde in PBS, all coverslips were rinsed with a saline solution [150 mM NaCl/4.2 mM KCl/2 mM $CaCl_2$/0.7 mM $MgCl_2$/10 mM Tris/HCl (pH 7.4)]; some were incubated for a further 10 s with an isotonic high-KCl buffer [5 mM NaCl/105 mM KCl/2 mM $CaCl_2$/0.7 mM $MgCl_2$/10 mM Tris/HCl (pH 7.4)] to depolarize the cells [17] and increase the intracellular Ca^{2+} concentration.

Immunoblot and immunofluorescence experiments

As primary antibodies, polyclonal anti-S100A1 antibodies were generated by immunizing rabbits with purified recombinant S100A1. Antibodies were affinity-purified on S100A1–Sepharose and eluted with 0.1 M glycine, pH 2.5, and neutralized immediately with 0.1 vol. of 1 M Tris/HCl, pH 9.2. In immunoblot experiments of rat tissues, this antibody at 2 μg/ml had the expected tissue profile [18] and did not cross-react with nine other S100 proteins including S100A6 or S100B (the S100 proteins most closely related to S100A1) or other EF-hand proteins tested (results not shown). The following anti-synapsin antibodies were used: monoclonal antibodies 10.22 against synapsin Ia/b, and 19.4(I) specific for synapsin IIa/b [19]; rabbit polyclonal G-143 specific for the dephospho form and G-257 for the phospho form of site 1 in synapsins I and II [20]. In immunoblots, the antibodies were used at 1:2000 dilution for detection with horseradish-peroxidase-conjugated secondary antibodies (Dako) and enhanced chemiluminescence reagents (Amersham). For immunofluorescence, coverslips were incubated with the affinity-purified anti-S100A1 antiserum and the anti-synapsin IIa/b monoclonal at 1:100 dilution for 60 min, followed by 1:200 anti-rabbit/Texas Red (Molecular Probes) and anti-mouse/Alexa 488 (Molecular Probes) conjugates. Double-labelled cells were analysed with a laser confocal microscope (Bio-Rad MRC 1024).

RESULTS

Identification of synapsins as Ca^{2+}/S100A1-binding proteins

Rat brain lysates were applied to an S100A1–Sepharose column in the presence of 1 mM $CaCl_2$, 100 μM $ZnCl_2$ and 0.1 % (v/v) Tween 20. After several washes, the column was eluted in a similar buffer containing 5 mM EGTA to chelate the Ca^{2+}. The

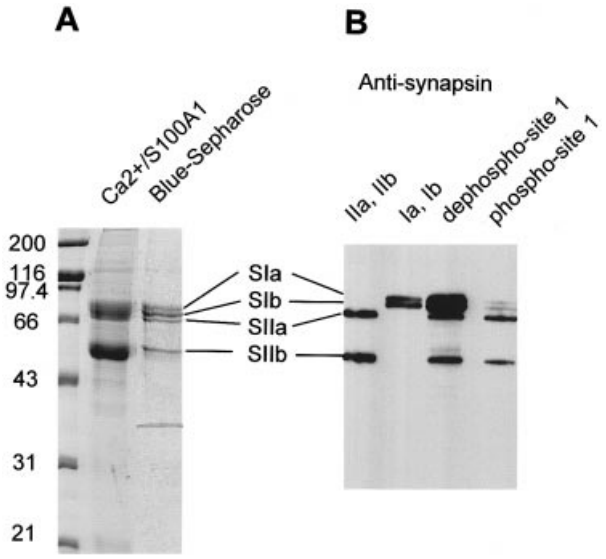

Figure 1 Identification of synapsins as Ca^{2+}/S100A1-binding proteins

(**A**) Coomassie Blue-stained SDS/12% (w/v) polyacrylamide gel of proteins purified from brain by Ca^{2+}-dependent S100A1-affinity chromatography and Blue-Sepharose chromatography as indicated at the top. Molecular mass standards are shown at the left (in kDa). The apparent band at approx. 38 kDa in the Blue-Sepharose lane does not show protein but a crack in the gel. (**B**) Immunoblot analysis of the Ca^{2+}/S100A1-affinity-purified fraction with monoclonal antibodies against synapsin IIa/b (SIIa, SIIb) and synapsin Ia/b (SIa, SIb), and phosphorylation-state-specific polyclonal antibodies for site 1.

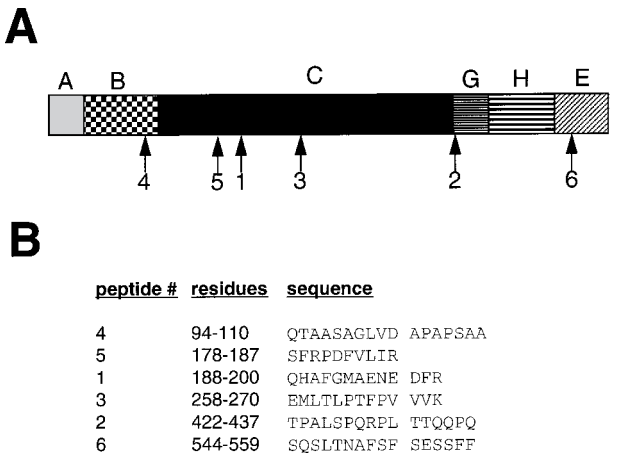

Figure 2 Microsequence analysis of purified synapsin IIa

(**A**) Schematic representation of the domain organization of synapsin IIa and the location of tryptic peptides. (**B**) Amino acid sequences of tryptic peptides and their positions in the synapsin IIa sequence.

eluted material was further purified using a Blue-Sepharose column (which binds adenosine-cofactor-requiring proteins). Staining with Coomassie Blue revealed that this fraction contained four highly enriched proteins, which are already major components after S100A1-affinity chromatography (Figure 1A). One of these bands, with an apparent mass of approx. 74 kDa, was excised from the gel and subjected to a tryptic digest followed by matrix-assisted laser desorption ionization–time-of-flight MS and Edman degradation of isolated peptides for identification. Six peptide sequences were obtained with a total of 85 residues; all of these matched synapsin IIa (Figure 2). Whereas peptides 1–5 are also present in synapsin IIb, peptide 6 was specific for synapsin IIa because domain E is absent from the alternatively spliced IIb isoform [21].

The electrophoretic mobilities of the other three purified proteins suggested that they represent synapsins Ia, Ib and IIb. This hypothesis was confirmed by immunoblot analysis of the purified protein fraction with monoclonal antibodies against synapsin Ia and Ib and against synapsin IIa and IIb respectively (Figure 1B). All four proteins reacted with a polyclonal antibody specific for the dephospho form of the cAMP-dependent protein kinase and calmodulin-dependent protein kinase I substrate site 1 (Ser-9 or Ser-10 in synapsin I or II respectively). Synapsin IIa and IIb, but not the synapsin I isoforms, also reacted with an anti-(phospho site 1) antibody (Figure 1B). This result probably reflects differential phosphorylation states of these proteins in the brain preparations used, rather than modulation of the S100A1 affinity by phosphorylation (see below). Notably, partially purified synapsin IIa expressed in baculovirus-infected insect cells had a chromatographic profile similar to that of the brain protein (Figure 3). This indicated that the synapsins were directly responsible for the binding, rather than being complexed by a minor S100A1-binding protein undetected by Coomassie staining.

Microsequence analysis revealed that the approx. 52 kDa band (located just below synapsin IIb in Figure 1A) present in the Ca^{2+}/S100A1-binding fraction, but not the Blue-Sepharose fraction, contained α- and β-tubulin (α-tubulin residues 353–370, VGINYQPPTVVPGGDLAK; β-tubulin residues 163–174, IMNTFSVMPSPK), which have previously been reported to interact with S100 proteins *in vitro* [2].

Synapsins as ATP-binding proteins

The purified synapsins were labelled with the ATP analogue FSBA to test by an independent method that their binding to Blue-Sepharose was due to the fact that they are nucleotide-

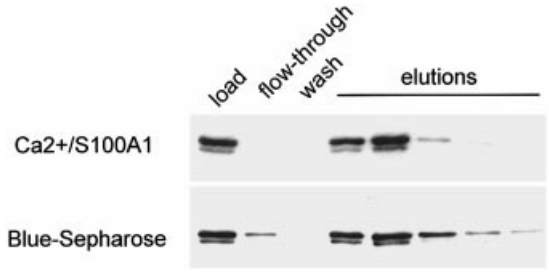

Figure 3 Chromatographic analysis of baculovirus-expressed synapsin IIa

Partly purified synapsin IIa extracted from the membrane fraction of baculovirus-infected Sf9 cells was subjected to Ca^{2+}-dependent S100A1-affinity chromatography followed by Blue-Sepharose chromatography. Aliquots of the loaded material and the flow-through, wash and eluted fractions were analysed by SDS/PAGE and immunoblot analysis. The faster-migrating band underneath synapsin IIa is most probably a proteolytic degradation product of synapsin IIa.

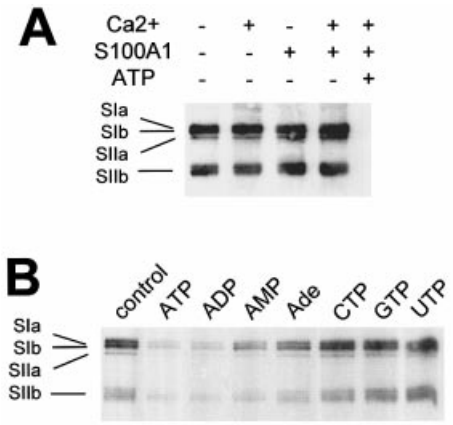

Figure 4 Labelling of the synapsins with FSBA

(**A**) Effect of Ca^{2+} and S100A1 on the labelling of the synapsins with FSBA, and competition by 2.5 mM ATP. (**B**) Competition experiments with adenosine (Ade) and various nucleotides (1 mM) as indicated at the top. Synapsin isoforms Ia to IIb (SIa, SIb, SIIa, SIIb) are indicated at the left.

binding proteins. Figure 4 shows that all four synapsins were labelled by FSBA. The labelling could be competed for by ATP and ADP, to a somewhat smaller extent by AMP and adenosine, but not by CTP, GTP or UTP (Figure 4B). However, labelling of the synapsins with FSBA was not modified by Ca^{2+} or S100A1 (Figure 4A).

Overall, these results are consistent with the recent crystallographic identification of synapsins as ATP-utilizing kinases similar to peptide-ligases such as glutathione synthase [22,23].

Ca^{2+}-dependent binding of S100A1 to immobilized synapsin

After demonstrating the binding of synapsins to immobilized S100A1 (Figures 1 and 3), we reciprocally tested this interaction by immobilizing the recombinant synapsin IIa on a biosensor chip in BIAcore surface plasmon resonance experiments (Figure 5). In these experiments, S100A1 bound to synapsin in the presence of Ca^{2+} (Figure 5A, broken line), but not in Zn^{2+} alone (dotted line), and the Ca^{2+}-dependent binding was enhanced by Zn^{2+} (solid line).

However, the kinetic analysis of the sensorgrams revealed that the interaction had at least two components with different on- and off-rates (results not shown). To analyse this bimodal interaction further, the following precautions were taken to minimize artifacts: first, the synapsin IIa (which was partly phosphorylated in insect cells) was dephosphorylated before being coupled to the chip surface; secondly, S100A1 was perfused at the maximal flow rate to prevent non-specific mass transfer; thirdly, S100A1 samples were determined as being homogeneously dimeric by gel filtration with a Superdex S200 column in a SMART system and were used in BIAcore experiments immediately after chromatography. This analysis revealed that the interaction was still biphasic at various S100A1 concentrations (Figure 5B) with off-rates of 0.012 and 0.195 s^{-1} respectively. The slow-off component accounted for more than 85 % of the total binding at all concentrations. Analysis of the real-time binding curves by using the slower off-rate revealed that the on-rate was inversely related to the concentration,

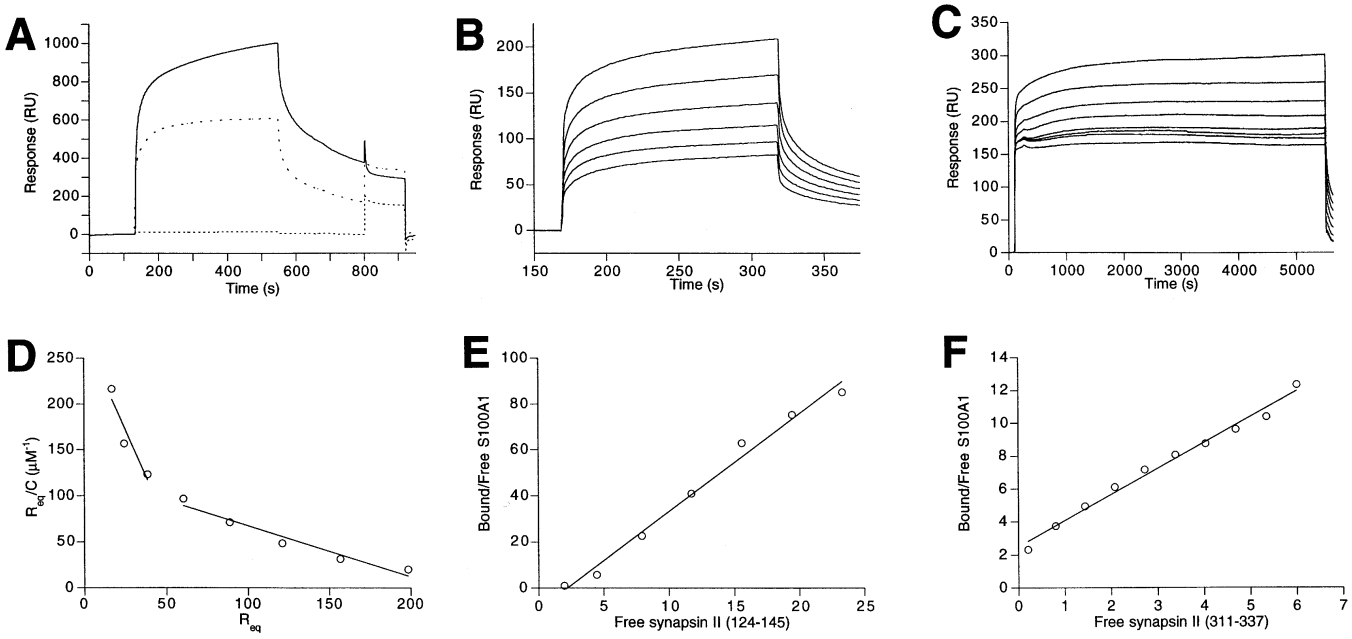

Figure 5 BIAcore experiments testing the interaction of S100A1 with immobilized synapsin IIa

(**A**) S100A1 (1 μM, 35 μl) was injected at 5 μl/min in the presence of 100 μM $ZnCl_2$ (dotted line), 1 mM $CaCl_2$ (broken line) or both 100 μM $ZnCl_2$ and 1 mM $CaCl_2$ (solid line). After the initial dissociation, the remaining S100A1 bound to the synapsin was completely stripped by injecting a buffer containing 5 mM EGTA at 800 s. (**B**) Sensorgrams showing 250 μl of S100A1 ranging in concentration from 156 nM to 5 μM injected at 100 μl/min for the kinetic analysis. (**C**) Injection of S100A1 (78 nM to 10 μM) at 2 μl/min over 90 min to estimate the equilibrium response. (**D**) Scatchard analysis of the data from (**C**) to determine the equilibrium binding constants of the S100A1 synapsin interaction: $K_{d1} = 245$ nM; $K_{d2} = 1.8$ μM. (**E**, **F**) Scatchard analysis of the dissociation constants of synthetic synapsin peptides: $K_d = 252$ nM (**E**); $K_{d1} = 660$ nM (**F**).

ranging from 7×10^3 to 5×10^4 $M^{-1} \cdot s^{-1}$ over the S100A1 concentration range 5 μM to 30 nM.

Two binding components were also indicated by Scatchard analysis (Figure 5D) of 90 min perfusions in which the endpoint was taken as approaching the response at equilibrium (Figure 5C), revealing a high-affinity component (K_{d1} = 245 nM) and a lower-affinity component (K_{d2} = 1.8 μM).

Competition of Ca^{2+}/S100A1 binding by synapsin peptides

Binding sites for S100 proteins, similarly to calmodulin-binding sites, do not have a canonical consensus sequence but are typically composed of a basic–amphiphilic α-helix [3,24]. In several proteins, calmodulin and S100 proteins can bind to the same site [12,24]. Two potential calmodulin-binding sites have been proposed for the C-domain of synapsins [25]. We therefore tested whether synthetic peptides containing these sequences could compete for Ca^{2+}/S100A1 binding to synapsin IIa.

Remarkably, a peptide containing synapsin II residues 124–145 (HTDWAKCFRGKKILGDYDIKVE) had an almost identical affinity for S100A1 (K_d 252 nM) to that of the high-affinity site (K_{d1} 245 nM) of the intact protein (Figure 5E). This sequence forms a loop in synapsin crystals [22]; it is conceivable that this loop could adopt a helical conformation on binding to Ca^{2+}/S100A1. The other peptide, containing residues 311–337 (AKYDIRVQKIGNNYKAYMRTSISGNW), also had a reasonable affinity for S100A1 (Figure 5F). However, the major part of this sequence forms a β-strand in the crystal structure [22], which casts some doubt on whether it could act as a binding site in the native protein, where it is more constrained than in a flexible peptide.

Cellular localization of synapsins and S100A1

To interact in neuronal cells *in vivo*, S100A1 and synapsins would need to have an overlapping subcellular localization. To analyse the localization of these proteins, we differentiated PC12 cells to a neuron-like phenotype by the addition of NGF for subsequent double-labelling immunofluorescence experiments. In our PC12 cells, S100A1 expression was maximal 3 days after the addition of NGF (Figure 6). Of the synapsins, synapsin IIa was the most abundant isoform, followed by synapsin IIb, both with maximal expression 3–4 days after the onset of differentiation, whereas there was hardly any synapsin I. In the immunoblots of crude PC12 cell lysates, the antibodies reacted only with the expected bands (Figure 6), demonstrating their usefulness for immunocytochemical studies. We therefore used the anti-synapsin II monoclonal antibody, in concert with the rabbit anti-S100A1 antiserum, for the immunofluorescence analysis of PC12 cells approx. 3.5 days after the addition of NGF. Because the interaction of S100A1 and synapsins is Ca^{2+}-dependent, some cells were depolarized with isotonic high-KCl buffer, to raise the intracellular Ca^{2+} concentration, immediately before the fixation. Figure 7 shows that S100A1 is present thoughout PC12 cells except the nucleolus, with a slightly stronger signal in the cytoplasm than in the nucleus (Figures 7A, 7D and 7G). In contrast, synapsin II is excluded from the nucleus and is highly localized to the soma and neurites (Figures 7B, 7E and 7H), where it has a distribution similar to that of S100A1 (Figures 7C and 7F). Although the overall subcellular distribution of S100A1 and synapsin II was not affected by depolarization, the localization of the two proteins in the neurites seemed to overlap more pronouncedly after depolarization (Figure 7F) than in non-depolarized cells (Figure 7I).

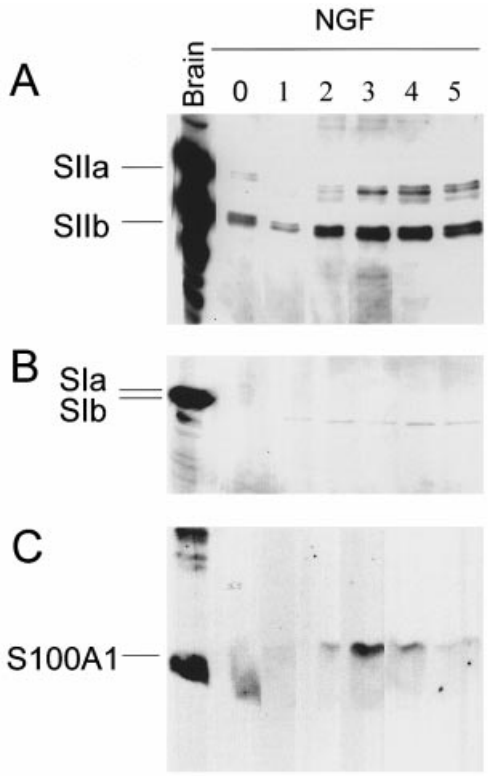

Figure 6 Immunoblot analysis of synapsins and S100A1 in PC12 cells

Immunoblot analysis of clarified PC12 cell lysates after the addition of 80 ng/ml NGF for 0–5 days, as indicated at the top. Total brain lysate is shown at the left. (**A**) Immunoblot probed with a monoclonal anti-[synapsin II (SIIa, SIIb)] antibody, 19.4(I). (**B**) Immunoblot probed with a monoclonal anti-[synapsin I (SIa, SIb)] antibody, 10.22. (**C**) Immunoblot probed with a polyclonal anti-S100A1 antibody.

DISCUSSION

The experiments described here demonstrate that synapsins and S100A1 can interact in a Ca^{2+}-dependent manner with high affinity *in vitro*. The synapsins and S100A1 also have a partly overlapping subcellular distribution in neuronal cells, indicating their potential to interact *in vivo*. A novel synapsin III isoform has recently been identified [26,27]. We did not specifically analyse the brain S100A1-binding protein fraction for the presence of synapsin III; the failure to detect it by Coomassie staining could be due to its low abundance compared with that of the synapsin I and II isoforms. As the C-domain of synapsin III is highly conserved with the synapsins I and II, synapsin III is also likely to interact with Ca^{2+}/S100A1.

The BIAcore experiments indicated a biphasic interaction of S100A1 and synapsin, with two equilibrium binding constants. There are several explanations for this observation, for example two S100A1-binding sites in synapsin, two synapsin-binding sites on S100A1 or a single binding site that has a lower affinity (fast-on/fast-off) during the initial docking step before the complex rearranges to a more stable interaction. The affinity of the synapsin II (124–145) peptide for Ca^{2+}/S100A1 is strikingly similar to that of the high-affinity site of the intact protein. This sequence therefore most probably represents the high-affinity binding site in the synapsin C-domain. The only other region predicted to have the propensity to form a basic amphiphilic α-helix (and thus the only other potential S100A1-binding site) was

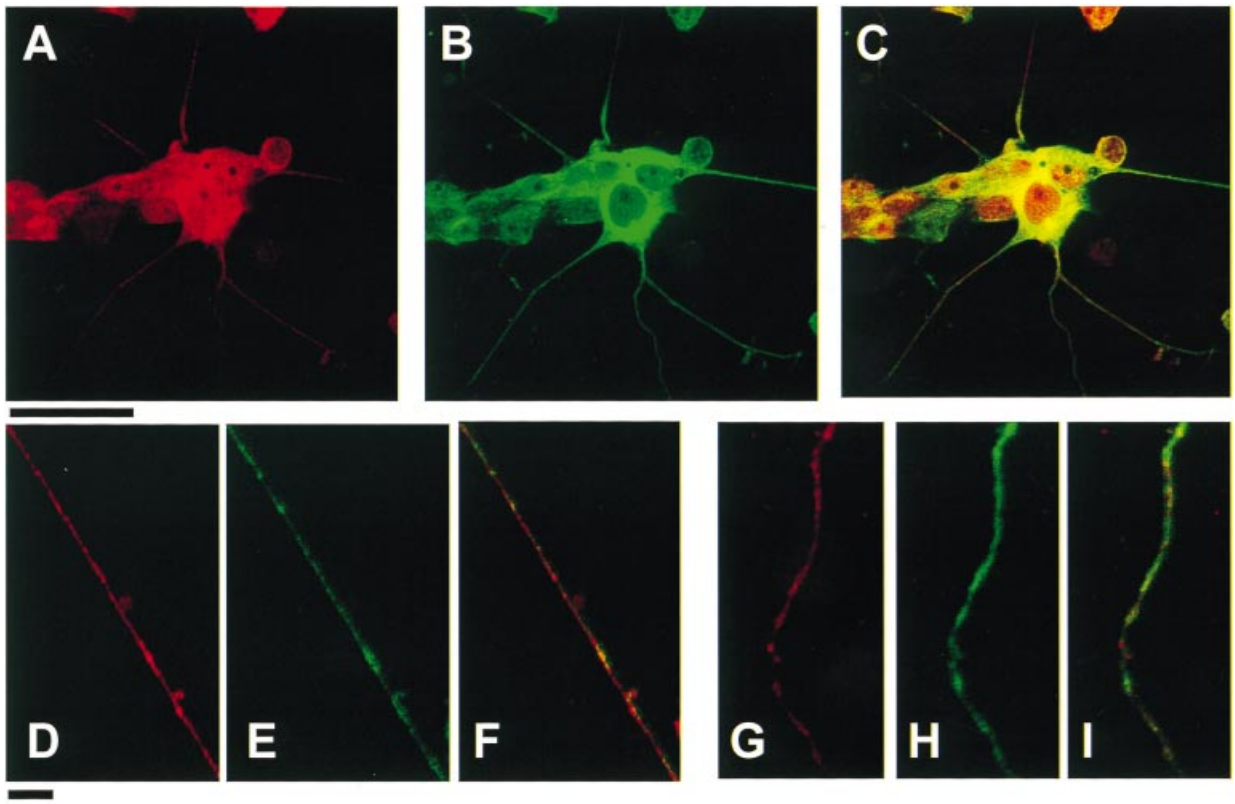

Figure 7 Localization of S100A1 and synapsin II in soma and neurites of PC12 cells

Confocal double-labelling immunofluorescence with the rabbit anti-S100A1 (red) (**A**, **D**, **G**) and monoclonal anti-(synapsin IIa/b) (green) (**B**, **E**, **H**) antibodies. Composite images are shown in (**C**), (**F**) and (**I**). (**A**–**F**) Cells were depolarized with an isotonic high-KCl buffer before fixation. (**G**–**I**) Neurite of a non-depolarized control cell. Scale bars, 50 μm (**A**–**C**) and 10 μm (**D**–**I**).

encompassed in the synapsin II (311–337) peptide [25]. This peptide also competed for the synapsin/S100A1 interaction with submicromolar affinity. However, despite the prediction for secondary structure, a major part of this sequence actually forms a β-strand in synapsin crystals [22]. This makes it unlikely that this sequence could interact with Ca^{2+}/S100A1, although there are other proteins in which the binding of effectors induces secondary structure changes (e.g. EF-Tu [28]).

At present it is unclear how synapsin function (and which one) could be modulated by Ca^{2+}/S100A1 binding. In synapsin crystals, two C-domains form tight dimers [22]; in the crystal symmetry, two such dimers form tetramers [22]. Interestingly, the major part of the tetramerization interface is formed by the four S100A1-binding sites. Ca^{2+}/S100A1 (and Ca^{2+}/CaM binding at the same site) could therefore have a role in shifting the equilibrium from tetramer to dimer; however, the significance of such a function is unclear. All proteins with a fold similar to that in synapsin are peptide ligases requiring ATP as a cofactor [29,30], for example glutathione synthase, but it is not known whether the synapsins have a similar activity. On the basis of the FSBA assays, S100A1 does not affect the ATP-binding activity of synapsin. This is conceivable in view of the synapsin crystal structure in which the nucleotide binding site is located in a wide open pocket that does not have direct contacts with the S100A1/calmodulin-binding site [22]. However, protein kinases such as smooth-muscle or skeletal-muscle myosin light-chain kinase, which require Ca^{2+}/calmodulin for activity, can similarly be labelled with FSBA in the absence of Ca^{2+}/calmodulin [31,32]. Therefore the fact that the FSBA labelling is independent of Ca^{2+}/S100A1 does not exclude the possibility that S100A1 could have some role in the regulation of the currently unknown catalytic activity of the synapsins.

We thank Dr. Mark Lam for help with the confocal microscopy, Dr. Martin Lackmann for advice on the biosensor experiments and analysis, Dr. Bostjan Kobe and Dr. Galina Polekhina for structural discussions, and Dr. Fabio Benfenati for providing the synapsin IIa baculovirus construct. This work was supported by the Deutsche Forschungsgemeinschaft (DFG) (J.H.), the National Health and Medical Research Council (NHMRC) of Australia (J.H. and B.E.K.) and USPHS grant MH39327 (P.G.). J.H. holds an NHMRC R. D. Wright award.

REFERENCES

1 Schäfer, B. W. and Heizmann, C. W. (1996) Trends Biochem. Sci. **21**, 134–140
2 Zimmer, D. B., Cornwall, E. H., Landar, A. and Song, W. (1995) Brain Res. Bull. **37**, 417–429
3 Heierhorst, J., Kobe, B., Feil, S. C., Parker, M. W., Benian, G. M., Weiss, K. R. and Kemp, B. E. (1996) Nature (London) **380**, 636–639
4 Kobe, B., Heierhorst, J., Feil, S. C., Parker, M. W., Benian, G. M., Weiss, K. R. and Kemp, B. E. (1996) EMBO J. **15**, 6810–6821
5 Südhof, T. C. (1995) Nature (London) **375**, 645–653
6 Chin, L. S., Ferreira, A., Kosik, K. S. and Greengard, P. (1995) Proc. Natl. Acad. Sci. U.S.A. **92**, 9230–9234
7 Li, L., Chin, L. S., Shupliakov, O., Brodin, L., Sihra, T. S., Hvalby, O., Jensen, V., Zheng, D., McNamara, J. O., Greengard, P. and Andersen, P. (1995) Proc. Natl. Acad. Sci. U.S.A. **92**, 9235–9239
8 Rosahl, T. W., Spillane, D., Missler, M., Herz, J., Selig, D. K., Wolff, J. R., Hammer, R. E., Malenka, R. C. and Südhof, T. C. (1995) Nature (London) **375**, 488–493
9 Ferreira, A., Chin, L. S., Li., L., Lanier, L. M., Kosik, K. S. and Greengard, P. (1998) Mol. Med. **4**, 22–28
10 Pieribone, V. A., Shupliakov, O., Brodin, L., Hilfiker-Rothenfluh, S., Czernik, A. J. and Greengard, P. (1995) Nature (London) **375**, 493–497

11 Hilfiker, S., Schweizer, F. E., Kao, H.-T., Czernik, A. J., Greengard, P. and Augustine, G. J. (1998) Nat. Neurosci. **1**, 29–35
12 Heierhorst, J., Mann, R. J. and Kemp, B. E. (1997) Eur. J. Biochem. **249**, 127–133
13 Siow, Y. L., Chilcote, T. J., Benfenati, F., Greengard, P. and Thiel, G. (1992) Biochemistry **31**, 4268–4275
14 Mitchelhill, K. I., Michell, B. J., House, C. M., Stapleton, D., Dyck, J., Gamble, J., Ullrich, C., Witters, L. A. and Kemp, B. E. (1997) J. Biol. Chem. **272**, 24475–24479
15 Ward, L. D., Howlett, G. J., Hammacher, A., Weinstock, J., Yasukawa, K., Simpson, R. J. and Winzor, D. J. (1995) Biochemistry **34**, 2901–2907
16 Lackmann, M., Mann, R. J., Kravets, L., Smith, F. M., Bucci, T. A., Maxwell, K. F., Howlett, G. J., Olsson, J. E., Vanden Bos, T., Cerretti, D. P. and Boyd, A. W. (1997) J. Biol. Chem. **272**, 16521–16530
17 Zerby, S. E. and Ewing, A. G. (1996) J. Neurochem. **66**, 651–657
18 Kato, K., Kimura, S., Haimoto, H. and Suzuki, F. (1986) J. Neurochem. **46**, 1555–1560
19 Vaccaro, P., Dente, L., Onofri, F., Zucconi, A., Martinelli, S., Valtorta, F., Greengard, P., Cesareni, G. and Benfenati, F. (1997) Brain Res. Mol. Brain Res. **52**, 1–16
20 Czernik, A. J., Girault, J. A., Nairn, A. C., Chen, J., Snyder, G., Kebabian, J. and Greengard, P. (1991) Methods Enzymol. **201**, 264–283
21 Südhof, T. C., Czernik, A. J., Kao, H. T., Takei, K., Johnston, P. A., Horiuchi, A., Kanazir, S. D., Wagner, M. A., Perin, M. S., De Camilli, P. and Greengard, P. (1989) Science **245**, 1474–1480
22 Esser, L., Wang, C. R., Hosaka, M., Smagula, C. S., Südhof, T. C. and Deisenhofer, J. (1998) EMBO J. **17**, 977–984
23 Hosaka, M. and Südhof, T. C. (1998) J. Biol. Chem. **273**, 1425–1429
24 Baudier, J., Bergeret, E., Bertacchi, N., Weintraub, H., Gagnon, J. and Garin, J. (1995) Biochemistry **34**, 7834–7846
25 Nicol, S., Rahman, D. and Baines, A. J. (1997) Biochemistry **36**, 11487–14895
26 Kao, H. T., Porton, B., Czernik, A. J., Feng, J., Yiu, G., Haring, M., Benfenati, F. and Greengard, P. (1998) Proc. Natl. Acad. Sci. U.S.A. **95**, 4667–4672
27 Hosaka, M. and Südhof, T. C. (1998) J. Biol. Chem. **273**, 13371–13374
28 Polekhina, G., Thirup, S., Kjeldgaard, M., Nissen, P., Lippmann, C. and Nyborg, J. (1996) Structure **4**, 1141–1151
29 Dideberg, O. and Bertrand, J. (1998) Trends Biochem. Sci. **23**, 57–58
30 Galperin, M. Y. and Koonin, E. V. (1997) Protein Sci. **6**, 2639–2643
31 Kennelly, P. J., Colburn, J. C., Lorenzen, J., Edelman, A. M., Stull, J. T. and Krebs, E. G. (1991) FEBS Lett. **286**, 217–220
32 Kennelly, P. J., Leng, J. and Marchand, P. (1992) Biochemistry **31**, 5394–5399

Received 28 May 1999/9 August 1999; accepted 10 September 1999